

Project Title: Study of Coseismic Changes in Shear-Wave Splitting after the M6.7 Northridge Earthquake of 1994

USGS Grant: 97-GR03147

Principal Investigator: Yong-Gang Li

Institute: Department of Earth Sciences,
University of Southern California

Date: September 20, 1998

Final Report

I. Abstract

Three-component data from the Northridge aftershocks recorded at 11 portable stations are used for a systematic analysis of shear-wave splitting keyed to investigate the state of the tectonic stress in the epicentral area of the 1994 *M*6.7 Northridge earthquake. 9 stations were deployed roughly along a 30-km-long N-S line across San Fernando Valley (SFV) between the Santa Susana Mountains and Santa Monica Mountains. The line is about 7 km east of the Northridge epicenter. 2 stations were deployed in western SFV and Simi Valley west of the mainshock epicenter. Results show 20 to 130 ms shear-wave splitting for aftershocks occurring at depths between the surface and about 10 km. The time separation between the fast and slow shear waves increases progressively with the travel distance. The average shear-wave splitting is about 7 ± 2 ms/km, with greater value at shallower depth. However, the time separation remains nearly constant for events occurring at depths deeper than about 10 km. The preferred polarization direction of the fast shear wave is nearly N-S $\pm 20^\circ$, consistent with the direction of the regional maximum horizontal compressive stress but independent of the azimuth between the stations and events. We interpret that the shear-wave splitting is caused by microcracks and/or alternations aligned in the N-S direction. Because most events showing the increase of splitting time with travel distance are located in the hanging wall block of the Northridge thrust fault while the deeper events showing constant splitting time with travel distance are located in the Northridge primary rupture zone and foot wall block, we further interpret that cracks in the upper crust (hanging wall block) are vertical or sub-vertical but cracks in the lower crust (primary rupture zone and foot wall block) are horizontal or sub-horizontal. Observed shear-wave splitting is mainly attributed to vertical cracks in the hanging wall block while horizontal or sub-horizontal cracks in the primary rupture zone and foot wall block have no or less contribution to shear-wave splitting for nearly vertical incident *S* waves. The polarization of the fast shear waves recorded at surface stations depends on the anisotropy in the top layer.

Observations of shear-wave splitting in the Northridge epicentral area infer that the maximum horizontal principal stress is in the nearly N-S direction. The least principal stress is horizontal and in the nearly E-W direction in the upper crust (hanging wall block of the Northridge thrust fault), but it becomes vertical or sub-vertical in the lower crust where the Northridge earthquake occurred. Unruh et al. [1997] depicted the Northridge primary rupture zone to be ~5 km wide along the Northridge thrust fault below 7 km depth beneath San Fernando Valley by modeling geodetic surface deformation caused by Northridge aftershocks. They find that aftershock deformation in the primary rupture zone is consistent with slow continuation of the south-dipping reverse slip on the blind Northridge thrust fault while aftershock deformation in the hanging wall block can be characterized by horizontal E-W extension. Hauksson et al. [Fig. 9, 1995] showed that most aftershocks with thrust faulting mechanism occurred at depths deeper than 10 km beneath SFV while most events with strike-slip faulting mechanism occurred in the hanging wall block at the shallow depth, including the *M*5.1 aftershock occurring at ~2 km depth in northern SFV [Fig.6 and Table 2, Hauksson

et al., 1995]. Our observations of shear-wave splitting in the SFV area also infer that the state of stress in the Northridge hanging wall block is different from that in the primary rupture zone and foot wall block. The stress in the lower crust is dominated by the reverse-thrust or decollement faulting while the stress in the upper crust remains the regional strike-slip faulting.

While no strong evidence of post-earthquake changes in shear-wave splitting was found during several months after the Northridge mainshock, the plot of polarization directions of the fast shear waves shows a trend likely changing from N35°W to N5-10°E in the first 2 months after the main shock. However, the splitting rate was not changed during this time period, and remained 7 ± 2 ms/km. In 1997, we deployed 2 stations at the same sites in northern SFV to record aftershocks. The 1977 data show that the average polarization direction of the fast shear waves was still in N5-10°E, but the splitting rate decreased to 6 ± 2 ms/km, slightly smaller than that in 1994. Zhao et al. [1997] applied a stress inverse method to *P*-wave polarity data from Northridge earthquakes and found that the orientation of the principal pressure (*P*) axis was rotated westward 17° immediately after the mainshock and then rotated back to the original direction in the following 2 years. The shear-wave splitting data also infer that the direction of the maximum principal stress was rotated eastward 10°-15° in 2 months after the Northridge earthquake.

We then examined the three-component data recorded at 2 portable stations deployed in southern SFV/Santa Monica Mountains before the Northridge earthquake, which were originally for study of the site effect on the ground motion from local earthquakes. These 2 stations recorded the data from a cluster of foreshocks occurring in Santa Monica Bay during 10 days before the Northridge mainshock on January 17, 1995. The data show obvious changes both in the polarization directions and splitting rate between foreshocks and aftershocks occurring at the same places. The splitting rate was changed by a factor of ~30% from ~10 ms/km before the earthquake to ~7 ms/km after the earthquake. The polarization direction of the fast shear waves from foreshocks was nearly E-W, parallel to the strike of the Santa Monica Mountains fault (SMMF) before the Northridge earthquake, but it was changed to nearly N-S in the first a few weeks after the mainshock and afterwards returned to nearly E-W. These observations suggest that the state of stress around the SMMF could be affected by rapid release of the stress on the Northridge blind thrust fault during the mainshock. However, it is not conclusive because there are not enough three-component data recorded in the Northridge epicentral area from foreshocks for a systematic study.

II. The Data

We used three-component data from Northridge aftershocks recorded at portable stations in the epicentral area for shear-wave splitting analysis. After the *M*6.7 Northridge earthquake on January 17, 1994, a collaborative effort to record aftershocks was undertaken by several institutions led by the Southern California Earthquake Center (SCEC). In seven weeks after the mainshock, several tens of instruments were deployed in the epicentral area for different scientific purposes. The P.I. of this research project participated in the deployment of instruments and collected the data from the field.

In this research project, we selected 11 stations using REFTEK (Refraction Technology) recorders with three-component short-period velocity sensors (Mark product 1 Hz L4C). 9 stations (JFPP, LA00-03, SFMI, SFPW, SFYP, OVHS) were located roughly along a 30-km-long N-S line across the San Fernando Valley between the E-W striking Santa Susana Mountains to the north and the Santa Monica Mountains to the south (Figure 1). The line was sub-normal to the strike of the southwest-dipping Northridge thrust fault, and about 7 km east of the mainshock epicenter. This line was also sub-parallel to the San Fernando Lateral Ramp which is a left step on the east side of the Santa Susana thrust fault. Other 2 stations (CPCP, SMIP, BCDH) were located in the west part of the San Fernando Valley and the Semi Valley. These stations were operated for a few weeks to 3 months. The sensor at each station was buried with three-components aligned in vertical, N-S and E-W directions. Recorders worked for triggered events with the sample rate of 100, 200 or 250 samples per

second. The collected aftershock data were compiled in a completed data set available from the SCEC Data Center [Edelman and Vernon, 1996].

III. Analysis Methods

We use the displacement ratio method [Shih et al., 1989; Savage et al., 1989] to determine the polarization direction of the fast shear wave. This method has been used to analyze the shear-wave splitting data recorded in the Los Angeles basin for study of the regional stress regime [Li et al., 1994; Li, 1996]. In this method, the ratio of the total projections of particle displacements onto a pair of orthogonal axes in a time window including only the fast shear wave is calculated as a function of azimuth on a plane perpendicular to the direction of wave propagation. When the total displacement of the projected azimuth being examined is most nearly parallel to the major axis of the elliptical particle motion, the ratio is maximized. Thus, the maximum displacement ratio indicates the azimuth of the most linear particle motion of the fast shear wave. This is similar to the coherence matrix method. For the near-vertical raypath, the ratio is calculated by projecting total particle displacements of the two horizontal components onto trial axes oriented from 0° to 180° in 5° increments. The optimal time window for calculation should start at the onset of the fast shear wave and end before the onset of the slow shear wave. We calculate the displacement ratio in a small time window and increase the window length until the polarity of the fast shear wave becomes unstable due to the inclusion of the slow shear wave arrival. We plot the displacement ratio in terms of petal lengths in rose diagram. The orientation of the longest petal indicates the polarization direction of the fast shear wave.

The time separation between the two split shear waves is estimated from the rotated seismograms, polarization diagrams and displacement ratio method. The polarization diagram of horizontal motions are plotted in a time window starting from the onset of the fast shear wave and ending after the onset of the slow shear wave. The direction of the linear projection following the first onset indicates the motion of the fast shear wave. After the onset of the slow shear wave, the linear projection changes into an orthogonal direction. The number of samples between the two onsets gives the time separation between split shear waves. We then use the displacement ratio method to confirm the time separation estimated by the polarization diagram. We first rotate the two horizontal components of seismograms to the fast and slow directions if the polarization direction determined in the previous procedure is not nearly N-S. Then, we advance the slow shear wave one sample (10 ms) at a time to calculate the displacement ratio and register the peak value for each time lag. When the slow shear wave arrival best matches the fast shear wave arrival (i. e. the phase difference between two shear waves is zero), the ratio has the maximum peak value, indicating the maximum linearity in particle motion. The time separation between the split shear waves equals the lag time. It is similar to the waveform cross correlation method. The length of the time window used in this study is 50 to 100 ms, about the half period of the seismic signal starting right before the onset of the fast shear wave.

IV. Results

We analyzed three-component data from aftershocks occurring within the shear-wave window of 11 stations. The shear-wave window is defined as the locus of propagation paths which subtend an incidence angle, $i_0 = \sin^{-1}(V_s/V_p) \sim 35^\circ$, where V_p and V_s are velocities of P -waves and S -waves in the vicinity of the surface. Within the shear-wave window, the affect of S - P conversion at the ground surface on shear-wave splitting observation can be avoided. In fact, we include those events that have take-off angles from the hypocenter between 35° and 55° because the ray at the surface become steeper due to the high velocity contrast at the sedimentary basin/granite basement contact. Locations of events are given by the Caltech/USGS Southern California Seismic Network Catalog. The depth range of events is between ~ 2 km and ~ 18 km, corresponding to the top and bottom of the Northridge aftershock zone beneath San Fernando Valley.

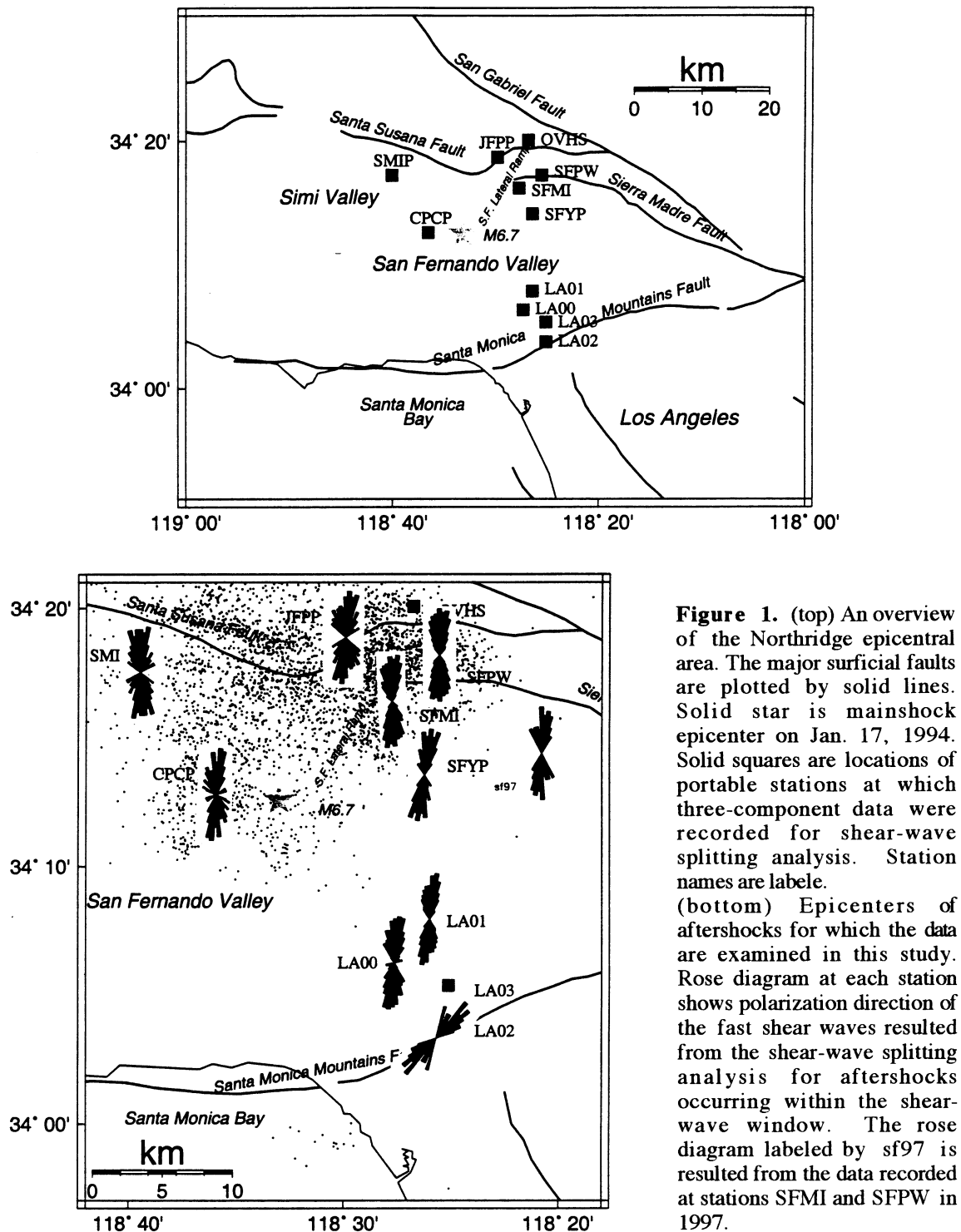


Figure 2a shows horizontal component seismograms recorded at station SFMI and results from shear-wave splitting analysis for 4 aftershocks occurring at depths of about 11 km with different azimuths to the station. Station SFMI was located near the San Fernando Lateral Ramp north of the Northridge Hill fault. We observe 90 to 120 ms splitting between the fast and slow shear-waves. Polarization directions of the fast shear waves are nearly N-S,

consistent with the direction of regional maximum principal stress but regardless of the azimuth between the epicenters and station. Further, Figure 2b shows shear-wave splitting for 8 aftershocks with different azimuths and focal depths between 6 km and 15 km. Again, we observe nearly N-S polarization directions of the fast shear waves for all these events. The separation time between the fast and slow shear waves increases from 60 ms to 120 ms as the depth increases from 6 km to ~11 km, but it remains almost constant for events occurring at depths deeper than about 11 km.

Figure 2a. (Left:) Horizontal components of seismograms recorded at station SFMI, from 4 aftershocks occurring at 10-12 km depths around the station with different azimuths between the events and station. The date of events is labeled at the top of the plot. Traces are labeled by the station name followed by N or E, denoting the N-S and E-W component, respectively. The data are cut arbitrarily in a 2-s time window. Zero does not correspond to the event initial time.

(Middle) Polarization diagrams and displacement ratio diagrams corresponding to seismograms. The time interval between dots in hodograms is 4 ms. The longest petal in displacement diagrams indicates the polarization direction of the fast shear wave. The step between petals is 5°. (Right) Plots of displacement (aspect) ratio vs. lag time. The peak displacement ratio corresponds to the time separation between the fast and slow shear waves.

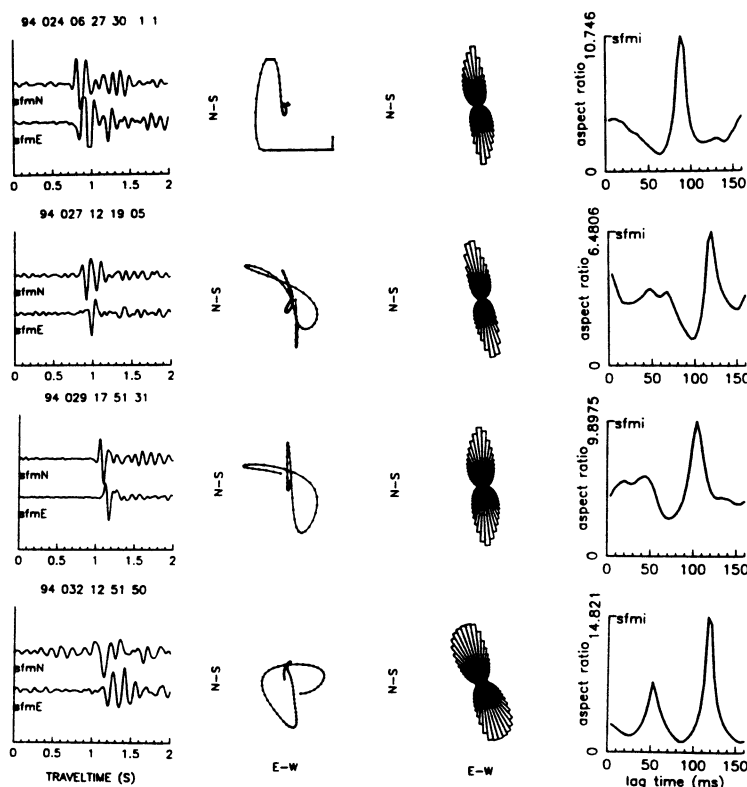


Figure 3 illustrates seismograms recorded at station SFPW located 5 km northeast of station SFMI for 9 aftershocks occurring at 5 to 15 km depths. Results from shear-wave splitting analysis for the data show that polarization directions of the fast shear waves are nearly N-S independent of the azimuth of events. The splitting increases from 30 ms to 120 ms as the focal depth increases from about 5 to 11 km, but no more increase happens to events occurring at depths deeper than ~11 km. Figure 4 shows the data recorded at station SFYP located 6 km southeast of station SFMI for 4 aftershocks occurring at 6 to 11 km depths. The splitting increases from 60 ms to 110 ms as the depth increases. Polarization directions of the fast shear waves are roughly in the N-S direction except for a few aftershocks occurring at deep level show northwestward polarization of the fast shear waves.

Figure 5 shows the shear-wave splitting recorded at stations LA00 and LA01 located at the south virgin of San Fernando Valley for 9 events occurring at depths between 8 km and 14 km. Again, polarization directions of the fast shear waves are nearly N-S regardless of the azimuth of events. The splitting increases from 60 ms to 130 ms as the depth increases, but no more increase for events occurring at depths deeper than about 13 km.

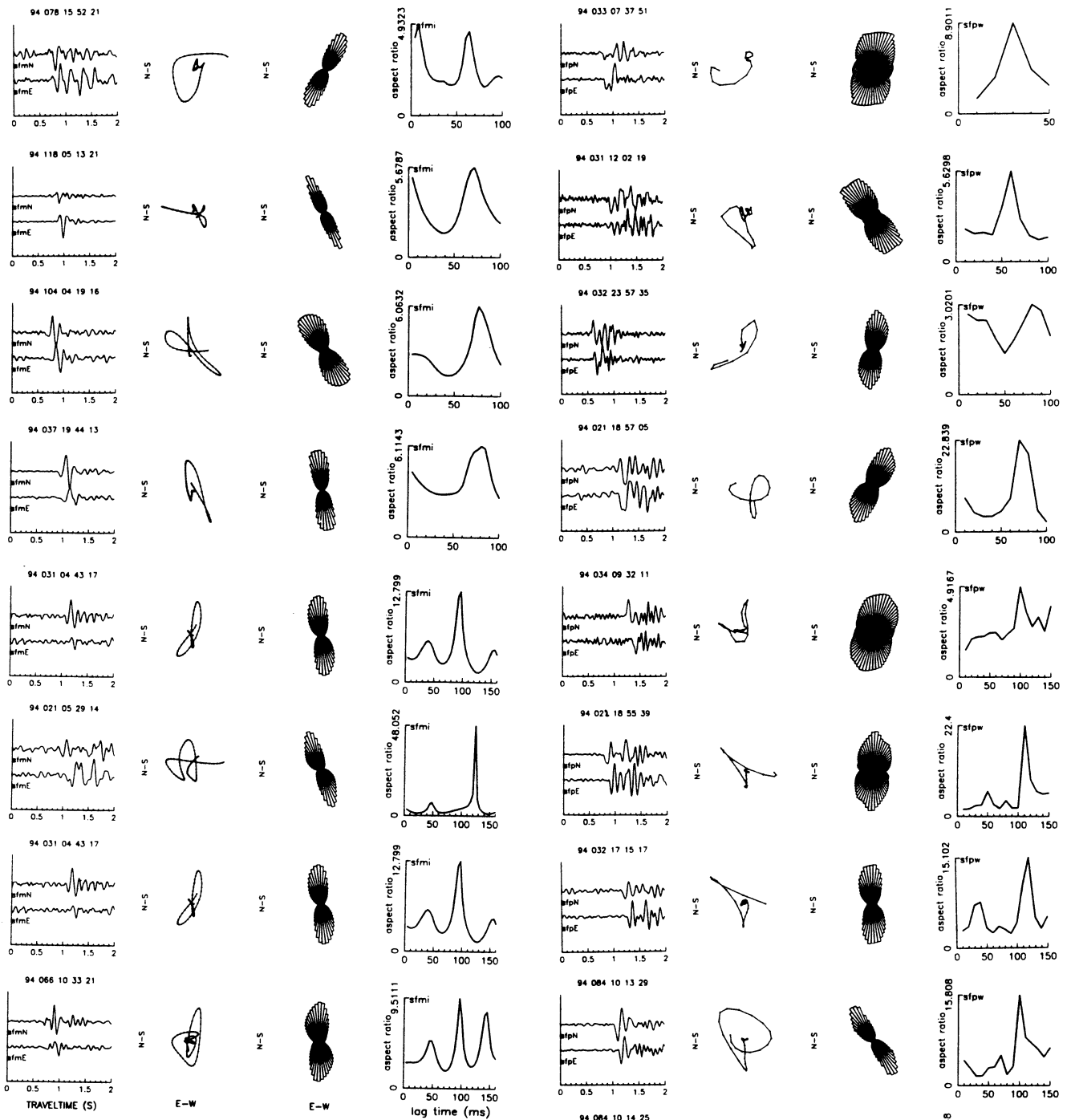


Figure 2b. Horizontal components of seismograms and shear-wave splitting analysis for 8 aftershocks occurring at depths of 6.1, 7.3, 9.2, 10.2, 12.8, 13.0, 13.7, and 15.0 km (from top to bottom) recorded at station SFMI. Note that the time scale in aspect ratio plot for deep events is different from that for shallow events. Other notations as in Fig. 2a.

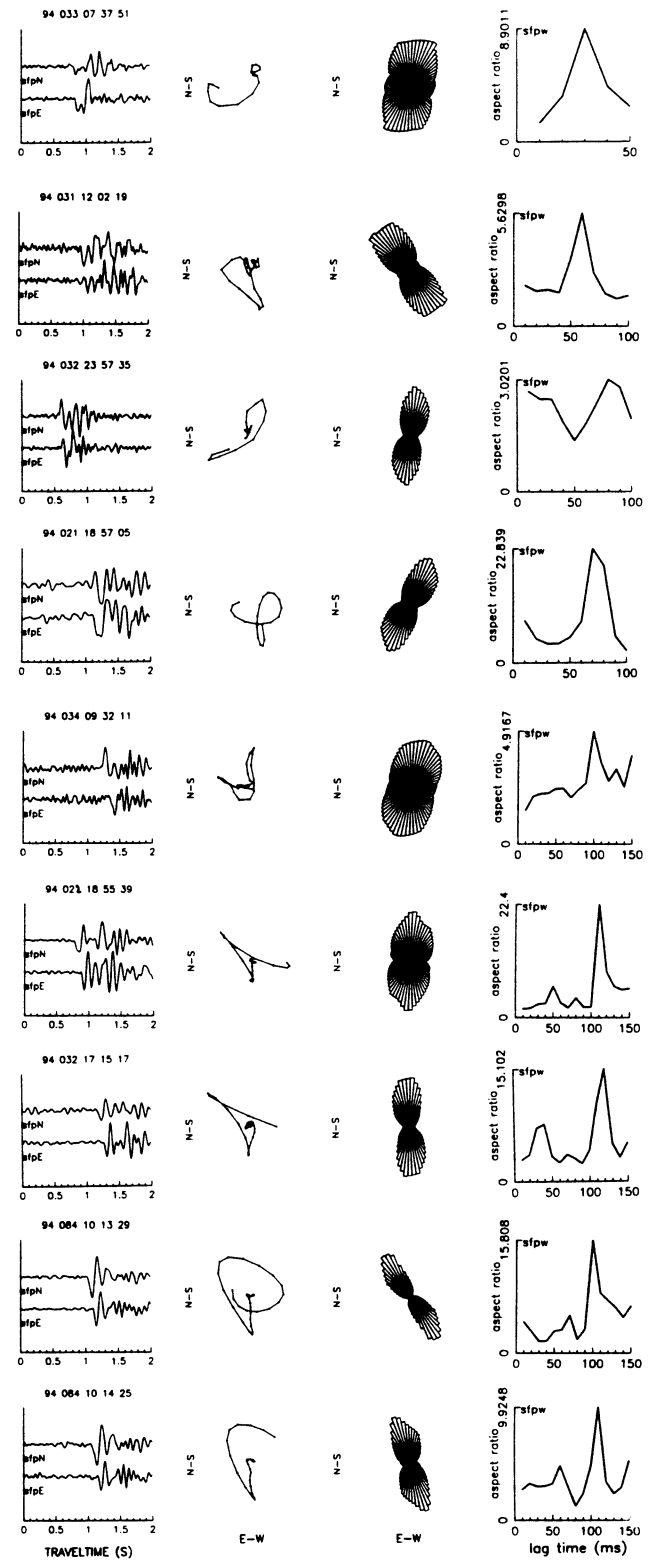


Figure 3 Horizontal components of seismograms and shear-wave splitting analysis at station SFPW from 9 aftershocks occurring depths of 5.3, 6.5, 7.4, 8.9, 11.0, 11.6, 13.8, 14.2 and 14.6 km. Other notations as in Fig. 2.

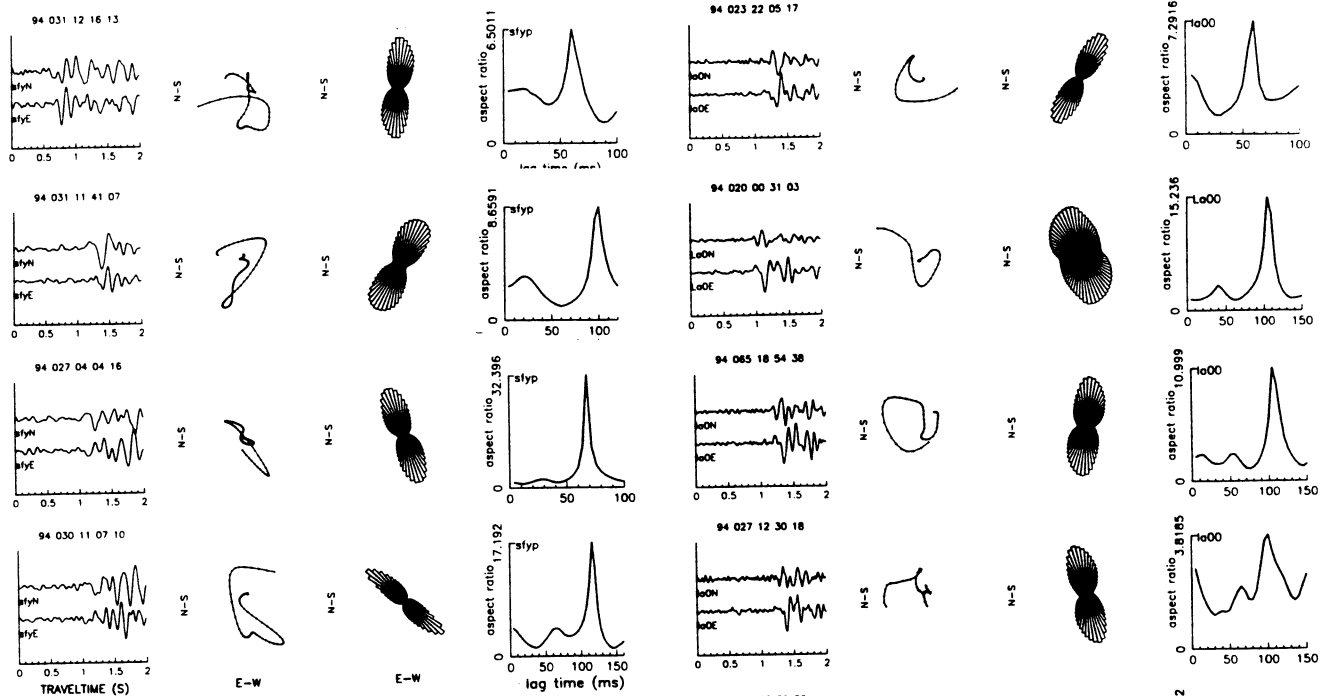


Figure 4. Horizontal components of seismograms and shear-wave splitting analysis for 4 aftershocks occurring at depths of 6.5, 8.8, 9.6, and 11.3 km (from top to bottom) with different azimuths and incident angles to station SFYP. Other notations as in Fig. 2.

Figure 5. Horizontal components of seismograms and shear-wave splitting analysis for 9 aftershocks occurring at depths of 8.3, 9.4, 10.3, 10.9, 12.4, 13.7, 13.8, 13.9, and 14.2 km (from top to bottom) recorded at stations LA00 and LA01 located in southern San Fernando Valley. The time interval between dots in hodograms is 5 ms. The delay time of the slow shear waves increases with depth. Other notations as in Fig. 2.

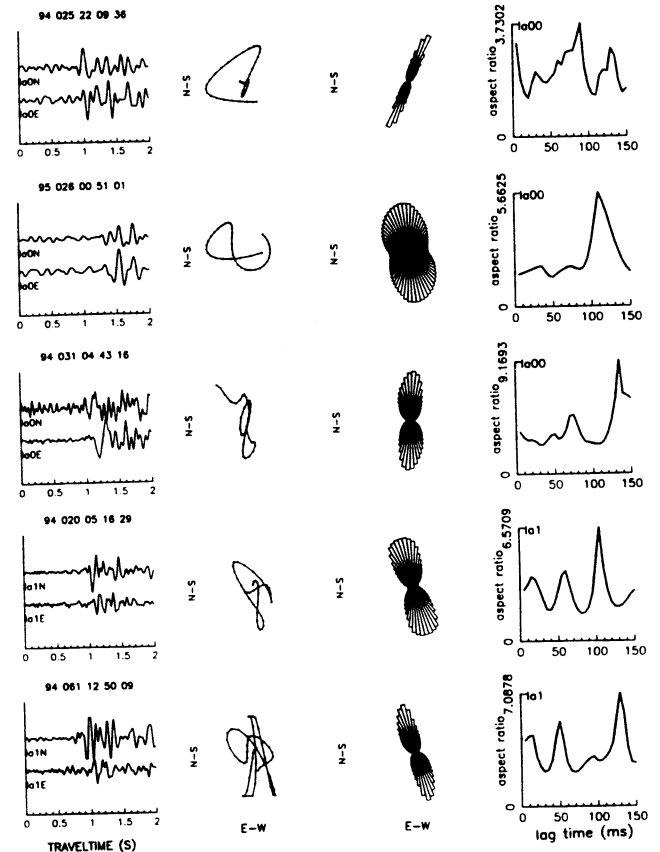


Figure 6 illustrates the data recorded at stations CPCP and SMIP located in the San Fernando Valley and Simi Valley west of the Northridge epicenter. We observed nearly N-S polarization direction of the fast shear waves at these two stations. Shear-wave splitting increases from 70 ms to 110 ms as the event depth increases from 5 km to ~10 km, but increases no longer for events occurring at depths deeper than ~10 km, including the event occurring at 21 km depth.

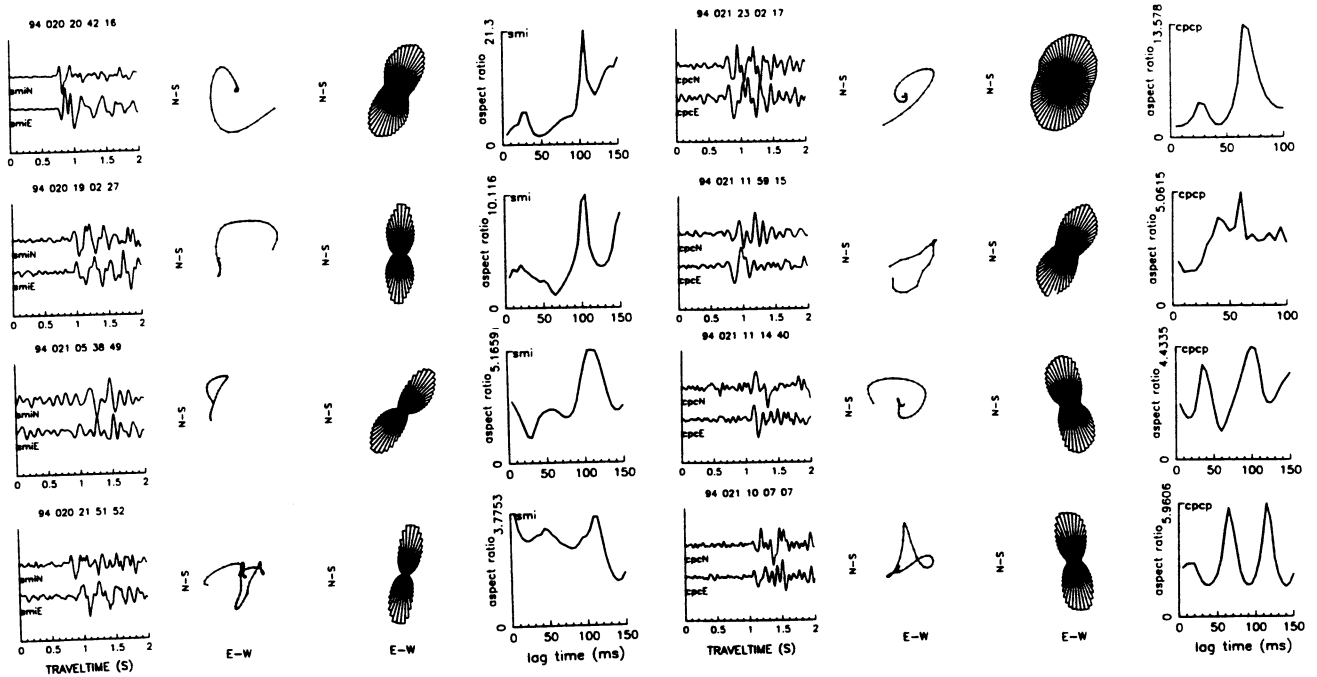


Figure 6. Horizontal components of seismograms and shear-wave splitting analysis for aftershocks recorded at station SMIP located in Simi Valley and station CPCP located in western San Fernando Valley. Focal depths of aftershocks registered at station SMIP are 9.8, 11.3, 14.0, and 21.0 km while focal depths of events registered at station CPCP are 5.0, 7.6, 11.2, and 14.4 km (from top to bottom). Other notations as in Fig. 5.

In order to examine the data systematically, we plot the results from shear-wave splitting analysis for all events recorded at each station. Figure 7a shows the rose diagram of polarization of the fast shear waves on the lower hemisphere out of 55° for the data from ~ 250 aftershocks recorded at station SFMI located in the northern San Fernando Valley. We find again that polarization directions of the fast shear waves from these events are consistently between $N-S \pm 15^\circ$, in spite of varying azimuths. We also plot time separations between the fast and slow shear waves versus the focal depths and travel distances between the station and these events. We find that the separation time increases as the travel distance increases for aftershocks occurring at depths shallower than about 10 km. However, the separation time remains almost constant for events occurring at depths deeper than ~ 10 km. The shear-wave splitting rate is around 7 ± 2 ms/km with greater rate at shallower depths, implying that the greater splitting is yielded in the sedimentary valley. We then plot polarization directions and shear-wave splitting rates versus the date for searching temporal variations in shear-wave splitting after the Northridge earthquake. Although the data are scattered, they show likely that the polarization direction of the fast shear waves was changed from $N355^\circ W$ to $N5-10^\circ E$ during the first 2 months after the mainshock on January 17 of 1994, and remained in this direction afterwards. However, no obvious change in shear-wave splitting rate is found during this period; it remained 7 ± 2 ms/km in about 3 months after the mainshock. In 1997, we deployed 2 portable stations at sites SFMI and SFPW for 3 months to record aftershocks. Figure 8 show example data recorded at these two stations in 1997. The results from shear-wave splitting analysis for the 1997 data are shown in Figure 7b. The average polarization direction of the fast shear waves remained in $N5-10^\circ E$ while the shear-wave splitting rate decreased to 6 ± 2 ms/km in 1997, slightly smaller than the shear-wave splitting observed at the same sites in 1994. This change in shear-wave splitting rate is also shown by example data in Figure 8.

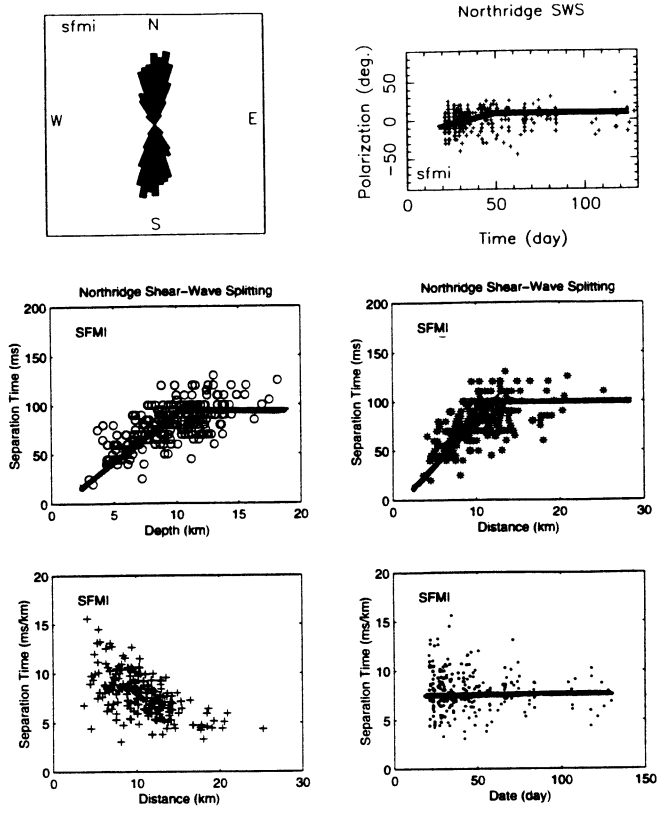


Figure 7a. Top: (left) The rose diagram of polarization on the lower hemispheres out of 55° for the data from ~ 250 aftershocks recorded at station SFMI in 1994. (right) Polarization directions of the fast shear waves versus date of events. Positive degree denotes the angle from north to east. Zero on the time axis denotes January 1st, 1994. The solid line is the least-squares fit to the data, showing a trend of changes in polarization direction with date. Middle: (left) Separation times between the fast and slow shear waves versus focal depths of events. (right) Separation times between the fast and slow shear waves versus travel distances between the station and events. The solid line is the least-squares fit to the data, showing a trend of changes in shear-wave splitting with depth and travel distance. Bottom: (left) Normalized separation times between the split shear waves versus travel distances. (right) Normalized separation times between the split shear waves versus date. The solid line is the least-squares fit to the data.

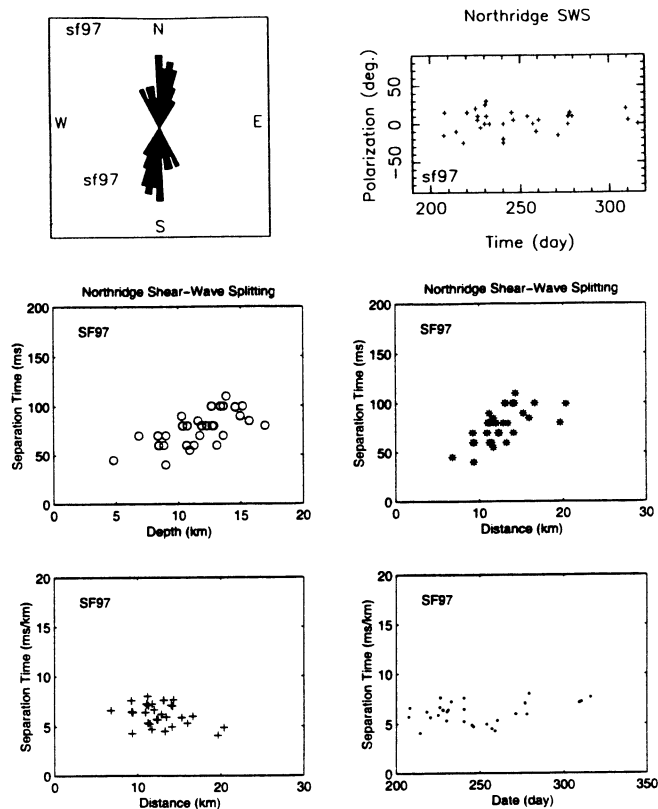


Figure 7b. Top: (left) The rose diagram of polarization on the lower hemispheres out of 55° for the data from 30 aftershocks recorded at stations SFMI and SFPW in 1997. (right) Polarization directions of the fast shear waves versus date of events. Positive degree denotes the angle from north to east. Zero on the time axis denotes July 19, 1997. Middle: (left) Separation times between the fast and slow shear waves versus focal depths of events. (right) Separation times between the fast and slow shear waves versus travel distances between the station and events. Bottom: (left) Normalized separation times between the fast and slow shear waves versus travel distances. (right) Normalized separation times between the fast and slow shear waves versus date.

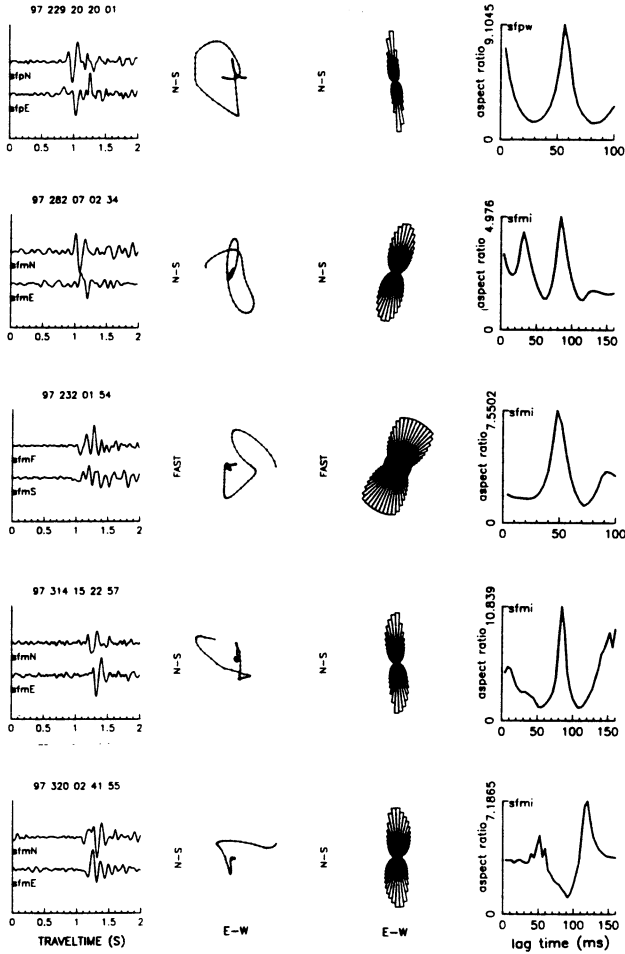


Figure 8. Horizontal components of seismograms and shear-wave splitting analysis for 5 aftershocks recorded at stations SMIP and SFPW in 1997. Focal depths of these events are 8.4, 10.3, 10.7, 11.6, and 13.8 km (from top to bottom). Locations of these events are close to those aftershocks occurring at the similar depths shown in Fig. 2. In general, separation times between the fast and slow shear waves from these events in 1997 are smaller than those from similar events in 1994. Other notations as in Fig. 2.

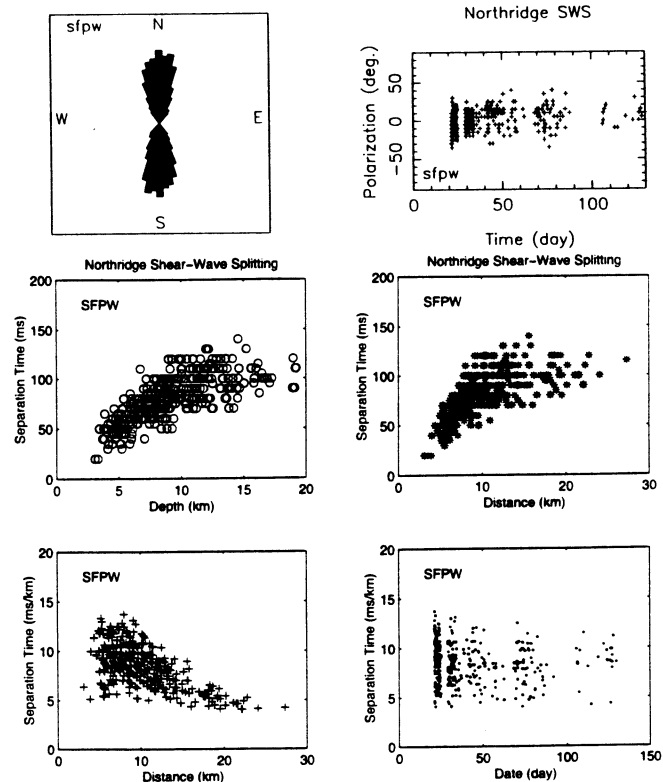


Figure 9. The plots of results from shear-wave splitting analysis for the data recorded at stations SFPW, LA00, LA01, JFPP, and SFYP. The station name is labeled in each plot. Top: (left) The rose diagram of polarization on the lower hemispheres out of 55° for the data from aftershocks recorded at station SFMI in 1994. (right) Polarization directions of the fast shear waves versus date of events. Positive degree denotes the angle from north to east. Zero on the time axis denotes January 1st, 1994. Middle: (left) Separation times between the fast and slow shear waves versus focal depths of events. (right) Separation times between the fast and slow shear waves versus travel distances between the station and events. Bottom: (left) Normalized separation times between the split shear waves versus travel distances. (right) Normalized separation times between the split shear waves versus date.

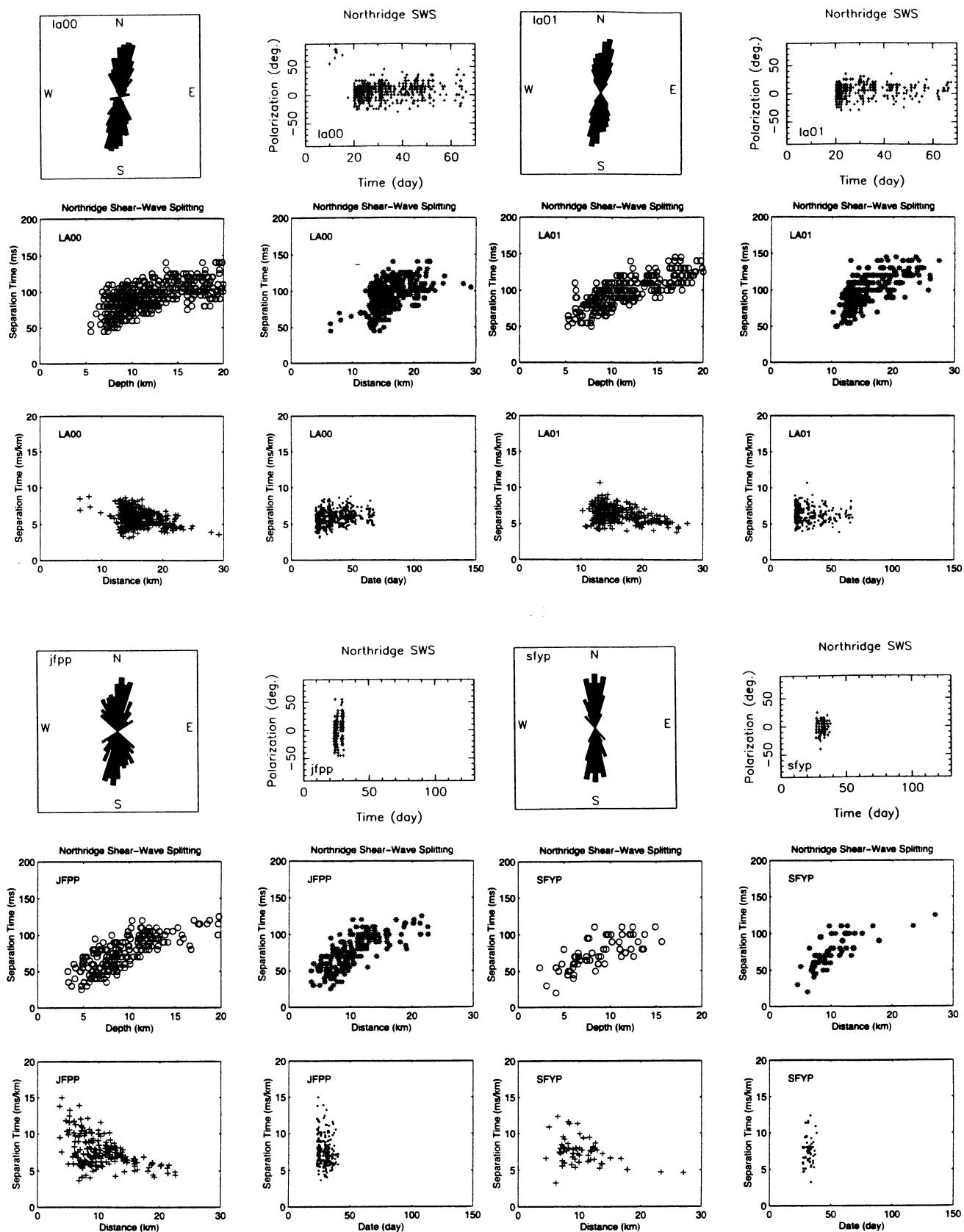


Figure 9. (continue) The plots of results from shear-wave splitting analysis for the data recorded at stations SFPW, LA00, LA01, JFPP, and SFYP.

In summary, we plot results from shear-wave splitting analysis for the data recorded at 10 portable stations deployed in the Northridge epicentral area. The rose diagrams showing polarization directions of the fast shear waves at these stations are plotted in Figure 1. The preferred polarization direction of the fast shear wave is nearly N-S $\pm 20^\circ$ at all these station. Figure 9 shows the complete results from the data recorded at stations SFPW, LA00, LA01, JFPP and SFYP. Generally, the results from these stations are the same as those from station SFMI shown in Figure 7. Polarization directions of the fast shear waves are consistently in nearly N-S, independent of varying azimuths between the stations and aftershocks. The separation time between the split shear waves increases as the travel distance increases for aftershocks occurring above 10 km depth, with the greater increase rate at shallower depth, suggesting that the anisotropy of the sedimentary rock in the San Fernando Valley is stronger than the basement crystalline rock. Most of these events occurred in the hanging wall block of the Northridge thrust fault. However, the separation time remains nearly constant for aftershocks occurring at depths deeper than ~ 10 km. Most of these deep events occurred in the Northridge primary rupture zone and the foot wall block. We interpret that the shear-wave splitting is caused by crustal microcracks and/or alternations which aligned in N-S direction of the regional maximum principal stress. We further tentatively interpret that the state of stress in the primary rupture zone and foot wall block (lower crust) is different from that in the hanging wall block (upper crust). While the maximum horizontal principal stress in the San Fernando Valley area is in nearly N-S direction, consistent with the N-S compression tectonics in the region, the orientation of the least principal stress varies with depth. The least principal stress in the hanging wall block (upper crust) is horizontal and oriented in E-W direction, consistent with the regional strike-slip faulting. However, the least principal stress in the primary rupture zone and probably in the foot wall block (lower crust) becomes vertical or sub-vertical, corresponding to the reverse-thrust and/or decollement faulting on the Northridge blind fault. Microcracks contained in the hanging wall block are aligned preferably with the crack plan in vertical because the least principal stress is nearly horizontal there, but cracks contained in the primary rupture zone and/or foot wall are preferably horizontal or sub-horizontal because the least principal stress is nearly vertical there. The observed shear-wave splitting is mainly attributed to vertical cracks, but less contribution is given by horizontal cracks for nearly vertically incident *S* waves. The normalized separation times between the fast and slow shear waves show an average shear-wave splitting of 7 ± 2 ms/km in the hanging wall block (upper crust), with the greater value at the shallower depth. The data recorded at stations located in the southern San Fernando Valley/Santa Monica Mountains also show a relatively small shear-wave splitting. Using ray-tracing modeling for anisotropic media containing vertical cracks [Li et al., 1994; Li, 1996], we estimated the apparent crack density in the upper crust beneath San Fernando Valley to be $\sim 0.06-0.08$.

The shear-wave splitting data at stations SFPW, LA00, and LA01 also show a trend, probably the temporal change in polarization direction of the fast shear waves although the data are scattered. The polarization direction likely changed from N355^oW to N5-10^oE in the first 1-2 months after the Northridge mainshock. However, the data show no obvious temporal change in splitting degree during 3 months after the mainshock. We have no more data recorded at these stations afterwards.

However, we observed obvious changes both in polarization directions of the fast shear waves and in splitting degrees between the foreshocks and aftershocks occurring in the Santa Monica Bay and recorded at stations LA00 and LA02. Figure 1 shows locations of a cluster of foreshocks occurring during 10 days before of the Northridge mainshock. The polarization directions of these foreshocks registered at station LA00 are plotted in Figure 9, showing about 70^o rotation from sub-parallel to E-W to sub-parallel to N-S.

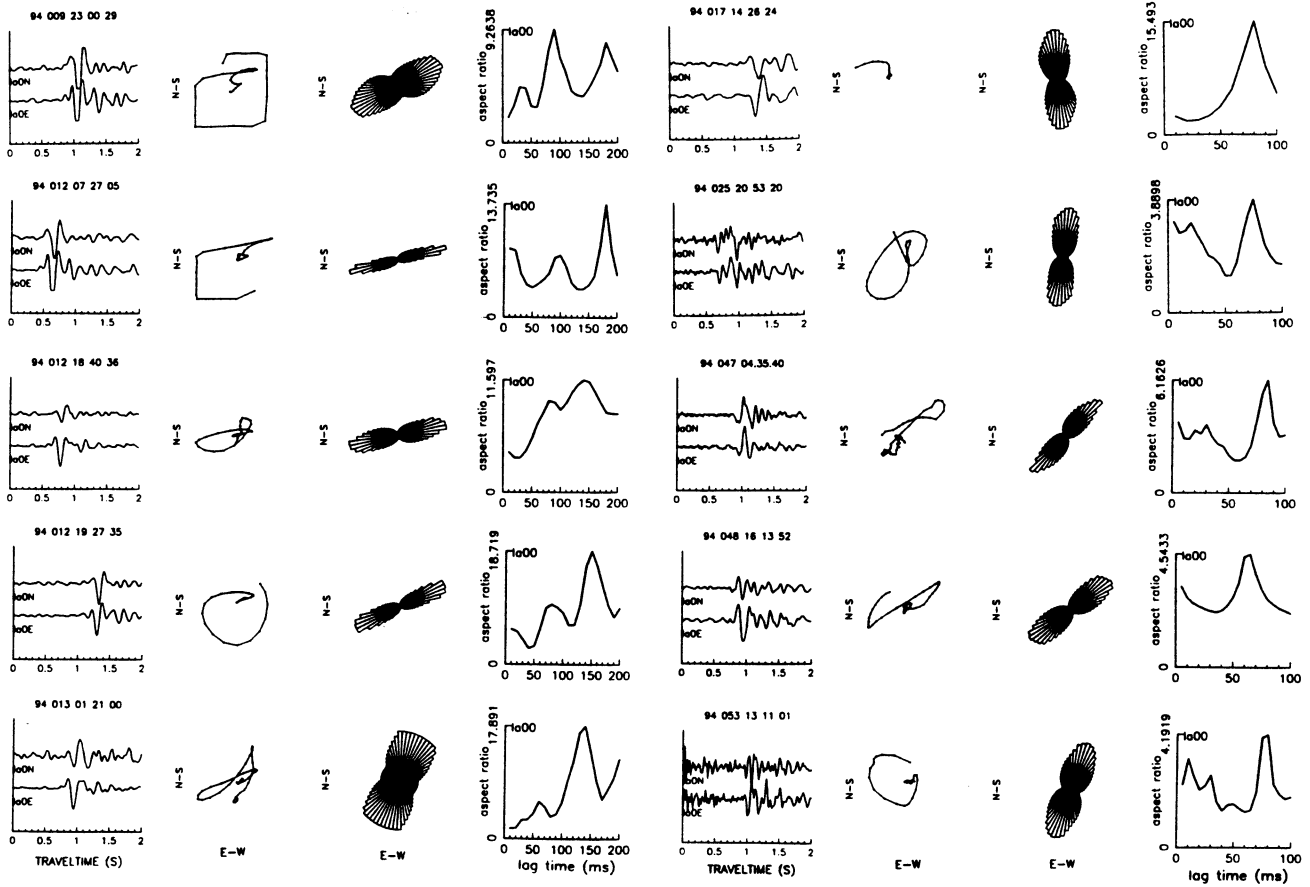


Figure 10. (left) Horizontal components of seismograms recorded at station LA00 and shear-wave splitting analysis for 5 foreshocks occurring at depths of 6.5, 11.0, 12.6, 11.7, 10.1 km in Santa Monica Bay during 10 days before the Northridge mainshock on Jan. 17, 1994. (right) Horizontal components of seismograms recorded at station LA00 and shear-wave splitting analysis for 5 aftershocks occurring at depths of 14.0, 12.6, 12.7, 9.5 and 8.5 km in Santa Monica Bay. The dates of these events are plotted in the title of each plot. Other notations as in Fig. 2.

Because raypaths between the station and these events transact the E-W striking Santa Monica Mountains fault (SMMF) which is a north-dipping reverse thrust fault, the fast shear waves might be polarized parallel or sub-parallel to the E-W strike of the fault. However, the rapid stress release on the Northridge thrust fault in the mainshock might cause the temporal change of the stress state on the neighboring faults, including the SMMF. Figure 10 shows seismograms and results from shear-wave splitting analysis for 5 foreshocks and 5 aftershocks occurring at depths about 11 km in the Santa Monica Bay. The average splitting decreased from ~ 10 ms/km before the earthquake to ~ 7 ms/km after the earthquake, changed by $\sim 30\%$. The polarization direction of the fast shear waves was changed from nearly E-W for foreshocks to nearly N-S in the first week after the Northridge mainshock, and then returned to nearly E-W afterwards. Because stations LA00 and LA01 were deployed only for a short time period before and after the Northridge earthquake and other portable stations were deployed after the mainshock, the data used in this study are not enough to achieve a solid conclusion for temporal changes in shear-wave splitting before and after the Northridge earthquake.